Article:

Ge, R, Ghadiri, M orcid.org/0000-0003-0479-2845, Bonakdar, T et al. (1 more author) (2017) 3D printed agglomerates for granule breakage tests. Powder Technology, 306. pp. 103-112. ISSN 0032-5910

https://doi.org/10.1016/j.powtec.2016.10.070

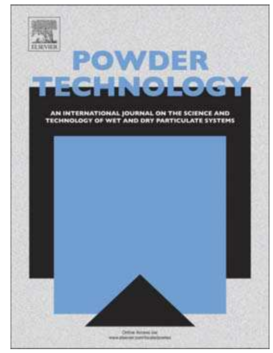

Accepted Manuscript

3D printed agglomerates for granule breakage tests

Ruihuan Ge, Mojtaba Ghadiri, Tina Bonakdar, Karen Hapgood

PII: S0032-5910(16)30764-1
DOI: doi: 10.1016/j.powtec.2016.10.070
Reference: PTEC 12069

To appear in: *Powder Technology*

Received date: 29 April 2016
Revised date: 28 September 2016
Accepted date: 31 October 2016

Please cite this article as: Ruihuan Ge, Mojtaba Ghadiri, Tina Bonakdar, Karen Hapgood, 3D printed agglomerates for granule breakage tests, *Powder Technology* (2016), doi: 10.1016/j.powtec.2016.10.070

3D Printed Agglomerates for Granule Breakage Tests

Ruihuan Ge[1], Mojtaba Ghadiri[2], Tina Bonakdar[2], Karen Hapgood[1*]

1 Monash Advanced Particle Engineering Laboratory, Department of Chemical Engineering, Monash University, Melbourne, VIC, 3800

2 Institute of Particle Science and Engineering, University of Leeds, UK

*Corresponding author: Karen.hapgood@monash.edu

Abstract

In the research into agglomeration, a long term barrier is the lack of a universally accepted method to evaluate the breakage propensity of agglomerates. Computer simulation is often used but is limited by the lack of identical, controlled agglomerates to test and validate simple models, let alone replicate the complex structure of real industrial agglomerates.

This paper presents work on the characterisation of strength of model test agglomerates prepared by a 3D printing production method enabling fully reproducible structures. Agglomerates were designed using Solidworks 2014 software and printed by an Objet500 Connex 3D printer. Materials with different mechanical properties were used to print the particles and the inter particle bonds, allowing a series of combinations of bond strength, particle strength and agglomerate structure to be tested. Compression and impact tests were performed to investigate the breakage behaviour of the printed agglomerates in terms of agglomerate orientations, bond properties and strain rates. This method will allow more rigorous testing of agglomerate breakage models.

Keywords: 3D printing; Agglomerates; Breakage test; PolyJet technology

1. Introduction

One of the long term barriers to advanced and accurate modelling of particulates is the lack of a suitable set of test particles that can be used to validate particle models. Generally the approach has been to take a specific, simplified particle system, measure the mechanical and surface properties as accurately as possible, and input these parameters into a model. The model is then used to estimate a property of the agglomerate – for instance agglomerate strength – and compared to experimental measurements on the simplified particle system. Whilst some of these approaches have produced some elegant simulation results, they often fail to produce an accurate prediction of the full distribution of behaviour of the simple particle system, let alone the behaviour of far more complex industrial powders.

There are two key limitations with the existing approach. Firstly, we collapse our experimental data to an average particle shape, average roughness, average surface energy etc. and eliminate the complexity of real particles very early in the process. The final model becomes "an average of averages", and the important effects of the structure, interactions and distributions are lost. Secondly, the destructive experimental tests can only ever test a single agglomerate in a single test condition and a single (usually unknown) orientation. The structural details of the agglomerate and the test conditions (particularly orientation) are never precisely modelled and the experimental test can never be replicated with an identical particle under identical conditions. Thus we are never sure if the model is insufficient to describe the behaviour, or if the model was accurate but the number of experimental testing replicates was insufficient to statistically converge to the average behaviour predicted by the model.

Real agglomerates produced by spray fluidised beds and high shear mixers in industrial processes have complex structures and irregular shapes which are difficult to study directly. At a basic level, general terms such as porosity or its complementary solid fraction are used to define the structure of the agglomerates [1-3]. These terms can also be related to variables such as coordination number or envelope density [4-6]. However, more advanced and useful analytic tools, such as X-ray microtomography technique, are recently available to study the structure of the agglomerates. Farber et al. [7] used X-ray microtomography to characterise pharmaceutical granules. Total porosity, pore size distribution and geometric structure were obtained by this technique. Rahmanian et al. [8] have also used X-ray microtomography to characterise the granule structure evolved in a high shear granulator. Due to complexity of the agglomerate breakage analysis in some cases, such as characterisation of internal stresses by experimental work, numerical simulation using Distinct Element Method (DEM) has been widely used by different researchers to provide a basis for sensitivity analysis of different factors affecting the agglomerate structure, and hence the breakage of agglomerates [9-11]. Golchert et al. [12, 13] for the first time studied the failure of the agglomerates with their structures characterised by X-ray micro-tomography, and their strength analysed by DEM models. The 3D spatial locations of particles of real agglomerates were obtained and implemented into the simulation code to generate simulated agglomerates. The effects of agglomerate shape and structure on breakage patterns during compression were analysed. A similar piece of work was carried out by Moreno-Atanasio et al. [14]. More recently, Dadkhah et al. [15, 16] characterised the internal morphology of agglomerates produced by a spray fluidised bed using X-ray micro-tomography. The 3D volume images of agglomerates were analysed in terms of porosity, coordination number, coordination angle. For the first time, they separated the solidified binder morphology of these agglomerates using this imaging technology. Although structural details of agglomerates can be obtained by X-ray micro-tomography, the destructive breakage tests can only be carried out on a single sample under a single orientation.

The effect of structure details has hardly been investigated and the breakage test can never be replicated under identical conditions. The complexity of the agglomerate structure, arising from different parameters such as primary particle size distribution, void fraction, inter-particle bond characteristics and material properties of both primary particles and bonds, makes it difficult to establish a full map of agglomerate breakage regimes. Overall, the agglomerates can break in different patterns, depending on their properties and loading conditions leading to various failure modes. Several pieces of work have been done on classification of patterns of agglomerate breakage [17, 18]. Subero and Ghadiri [17] made agglomerates using glass ballotini as primary particles bonded together by bisphenol-based epoxy resin. In order to explore the effect of agglomerate structure on agglomerate impact strength, the agglomerates were made with different levels of porosity by making different number and size of the macro-voids. The particles were impacted at different impact velocities and angles. In order to elucidate the fracture patterns, the shapes of the fragments were observed. They reported different patterns of breakage for agglomerate impact breakage obtained in their work, such as localised damage, fragmentation, multiple fragmentations with localised damage and disintegration. In order to study the effects of structure on agglomerate breakage, it is desirable to produce multiple identical test agglomerates with controlled structures, and then study their breakage behaviour in detail with the aid of mathematical models and experimental instruments.

In this study, 3D printer-Objet Connex 500 is used to print multiple customised agglomerates. The Objet 500 is an eight jet "PolyJet" printer which can print multiple materials simultaneously in a single print run, including rigid or rubber-like flexible materials with well-defined mechanical properties. Liquid photopolymer is printed on a build tray to form the object and cured with UV light. It can also print a removable support gel to support overhangs and/or complicated geometry. PolyJet prints simultaneously different materials with varied mechanical properties to represent the particles and/or dried liquid bridges between the particles. There are five broad material classes available, some with sub-variations: rigid opaque materials (2 variations); rubber-like materials (3 variations); transparent materials (2 variations); a polypropylene-like material and a high temperature material. The properties of each material are well defined and detailed datasheets are available [19], specifying density, hardness, tensile strength, elongation at break, elastic modulus, water adsorption and glass transition temperature T_g (where relevant), and other properties as well as the ASTM test method used to measure each of these properties. This permits a broad spectrum of agglomerates to be produced with "tuneable" physical properties.

Quasi-static compression tests and drop weight impact tests were carried out to investigate the agglomerate breakage behaviour at different strain rates. Preliminary experiments to determine the influence of agglomerate orientation, bond properties and strain rates were conducted to demonstrate "proof of principle" for the approach.

2 Methodology

2.1 Production process of agglomerates

Agglomerate models were designed by Solidworks 2014 software. The designed agglomerate models were exported in Standard Template Library (STL) file format before being imported to the Objet Connex 500 3D printer. The 3D printer uses PolyJet Matrix technology that can simultaneously print multiple materials with varied mechanical properties [19]. In this research, four different materials from "rubber-like" polymer material to a rigid material were used to print agglomerates. The mechanical properties of these materials are well characterised in a series of specification sheets [19] and are summarised in Table 1.

Figure 1 shows a typical 3D printing process. The STL format files of agglomerate models were loaded into the Object studio software. This software automatically places and orders the models on the build tray, and then starts the printing task on the Objet 3D printer. The print heads move repeatedly along X and Y axis, jetting the liquid polymers in 30 micron layers, which are cured by UV rays instantly. The material is deposited layer by layer until desired agglomerates are completed. During the printing process, a "waxy" support material is printed to support the complex structure of agglomerates, such as overhangs and internal gaps within the model.

<Table 1: Mechanical properties of 3D printing polymer materials>

<Figure 1: 3D printing process showing the printer, the software arranging the models to be printed, and the final product on the build tray.>

Two primary particle diameters of 3 mm and 4 mm were considered in this research. The corresponding doublet dimensions including bond thickness and length are shown in Figure 2. The white particles and the grey inter particle bonds in Figure 2 are defined in Solidworks as separate (but connected) objects and can be printed using different polymers as required. The inter-particle bond size is big enough compared to the 3D printing resolution, and also is suitable to facilitate the support removal process.

The agglomerate designs with 147 primary particles arranged in a simple cubic structure are shown in Figure 3. The agglomerates are printed layer-wise to produce a cubic structure at two different orientations on the build tray, referred to as "Print Orientation A" and "Print Orientation B", as shown in Figures 3 (a) and 3 (b). To illustrate the difference of these two different agglomerate printing orientations, the relative position of the internal simple cubic structure to the build tray is shown on the right side of the agglomerate design (see Figure 3).

Furthermore, these two orientations are printed with four bond types and two primary particle sizes. The agglomerates produced in different combinations are named as types I-IV, the details of which are given in Table 2.

<Figure 2: Schematic drawing of doublet>

<Figure 3: Agglomerate design in terms of different orientations>

<Table 2: Parameters of the tested agglomerates>

To obtain the final product, the support material of agglomerates shown in Figure 4 (a) must be removed. Due to the delicate structure of agglomerates, the high-pressure water jet cleaning method normally used for larger and stronger models cannot be used. The support material is described by the vendor as “waxy” but appears to be a complex polymer which does not have a melting point and is not soluble in water. The support removal progress appears to be influenced by many factors including temperature, pH and agitation. The agglomerates were soaked in a beaker containing a 2 % caustic soda solution, and then placed in a water bath and heated to 45-50 ^{o}C. This cycle was repeated several times to gradually dissolve the support material. The total cleaning time depends on the size and complexity of printed agglomerates but is generally in the order of several days to produce 20-40 clean and intact agglomerates. Figure 4 (b) shows the final agglomerates of different scales after removing support materials. As some agglomerates break during the cleaning process, more work is underway to determine the best method to remove the support material.

<Figure 4: Removal of support materials (a) printed agglomerates showing support material under the overhangs (b) various finished and cleaned agglomerates. >

2.2 Breakage test setup

In this research, primary particles were printed using a rigid polymer VeroWhitePlus^{TM}. In addition to this material, three other polymers were used to print the bonds between the primary particles, as given in Table 1.

3D printing builds the designs by applying successive 30 µm layers on top of each other to create the final structure. These printing layers can be seen when the agglomerate is examined closely with the naked eye. This suggests that the direction of the printing layers of agglomerate with regard to the applied load direction may affect the agglomerate strength. To investigate this possibility, different arrangements were used in breakage tests as shown in Figure 5. As shown in Figures 3 and 5, the agglomerates printed in the two different simple cubic arrangements are tested for their crushing strength. Each agglomerate is loaded in two directions also shown in Figure 5. The "loading direction 1" refers to the printed layers laid horizontally for testing and the agglomerate strength is measured with the applied load perpendicular to the printed layers. For the "loading direction 2", the agglomerate is rotated 90^o so that the printed layers are now vertical and parallel to the applied load direction.

<Figure 5: Different test directions and sample orientations used in breakage tests. Hatch lines within the particles indicate the direction of the 3D print layers. >

Compression tests were carried out to check the strength of printed agglomerates. Tests were conducted using an Instron 5566 universal testing machine with a 1 kN load cell and filmed using a Nikon D7000 camera. As shown in Figure 6 (a), the upper plate moves at a slow speed, and agglomerates are compressed between two rigid platens. A cross-head speed of 1mm/min was chosen to make sure the tests were in a quasi static state without impact effects. Four different agglomerate arrangements (see Figures 5a-5d) were considered during the compression tests and at least three replicates were performed for each experiment.

Drop weight impact testing was used to investigate the impact breakage behaviour of agglomerates at high strain rate. As shown in Figure 6 (b), the test was conducted by placing the sample on a flat anvil and dropping a weight onto the sample from a known height via an accelerating tube. In this study, the drop height was 1 m and three different drop weights were used: 0.2, 0.4 and 0.6 kg. The experiments were also filmed using a high speed camera with a

2000 f/s sampling rate. For the impact tests, two agglomerate arrangements were used (Figures 5a and 5c) and five replicates were performed for each experiment.

<Figure 6: Schematic of breakage test setups>

3 Results

3.1 Compression tests

Figures 7 and 8 show representative compression test curves for agglomerates prepared in Print Orientations A and B, and tested according to conditions shown in Figures 5(a) and (c), respectively. The results show good reproducibility for tests conducted under the same test conditions. The compression curves also show different behaviours when the agglomerate is compressed in parallel or normal direction with regard to orientation of printed layers. This is not just a matter of layer-wise printing but also the structure difference between Print Orientations A and B, where the former promotes slip along a "45^o plane", whilst the latter promotes tensile cleavage at "90^o plane", as it will be shown later on.

Figure 7 refers to the case where the agglomerate is prepared with "Print Orientation A" and tested under loading direction 1, i.e. having the printed layers horizontal and the applied load being vertical to the printed layer planes, as shown in Figure 5 (a). The breakage process can be divided into several stages. At low displacement, the bonds between primary particles mainly show elastic deformation. As the compressive load increases and reaches around 5 mm displacement, we see the onset of plastic deformation. After this critical point, extensive deformation takes place with little load changes, i.e. the agglomerate deforms plastically along the "45^o planes". Subsequently, with the increased displacement, the load increases to around 150 N at about 9-10 mm displacement. At this stage, the breakage is observed by a sudden drop in load. The spatial arrangement of the strong primary particles in such that compression is accommodated by slips along the "45^o planes". This can be observed from the camera stills.

In contrast, when the agglomerate is compressed according to the condition shown in Figure 5 (c), i.e. "Print Orientation B" with printed layers again perpendicular to the applied load direction, the load quickly rises with displacement and it reaches the first breakage at around 2 mm displacement, i.e. much less than the previous case, as shown in Figure 8. The camera stills reveal that, at this point, breakage occurs near the platen. After the first breakage point, additional breakage points are also observed. The camera stills illustrate that the agglomerate breaks gradually with the increased displacement. In this arrangement, the vertical planes are under tension, and hence horizontal bonds are easier to break along this plane.

<Figure 7: Force-displacement curves of agglomerates for condition of Figure 5 (a) (Agglomerate type I)>

<Figure 8: Force-displacement curves of agglomerates for condition of Figure 5 (c) (Agglomerate type I) >

The force-displacement curves of samples prepared with two different bond strengths for both Print Orientations A and B are shown in Figure 9. Test conditions for each agglomerate type correspond to Figure 5. It should be noted that the curve for the loading direction 1 in Figure 9 (a) is the same as Test 3 of Figure 7. This is also the case for Figure 9 (c), where horizontal direction curve is the same as Test 2 of Figure 8. Figures 9 (a) and 9 (b) show the bond strength difference on slip plane failure, whilst Figures 9 (c) and 9 (d) show the bond strength difference on tensile plane failure. Considering Figures 9 (a) and (b), the gross response is dominated by shear deformation on slip planes and hence the breakage curves show similar variation tendencies at the same bond strength and sample orientation. Figures 9 (c) and 9 (d) relate to the case where tensile stresses prevail on vertical planes parallel to the load, where failure is likely to be by tensile rupture.

The relative orientation of the printed layers with regard to the load direction is illustrated in Figure 10 for different experimental conditions. For "Print Orientation A" case, the bonds between primary particles are primarily under shear deformation for both loading directions, whilst for "Print Orientation B", the bonds experience tensile deformation at orthogonal orientation with respect to loading direction. It is noteworthy that the bond strength can be different with different printed layer directions, i.e. horizontal direction and vertical direction. To measure the individual inter-particle bond strength under different conditions, shear and tensile tests were performed on doublets made in purpose for it. For this experiment, two most different printing directions are considered. The results are given in Figure 11 and show that the bond strength is different for different printing layer directions. Especially, for agglomerate type II, the strength difference emanating from printed layer directions is more obvious. Therefore, for each Figures 9 (a) to 9 (d), the difference between the applied load direction with regard to the printed layers (i.e. load direction 1 and load direction 2) can be attributed to the strength difference of the printed bonds at different printing directions. Meanwhile, for all cases, the bond strength of agglomerate type II is always larger than that of agglomerate type I. As shown in Figure 9, the influence of bond strength on the compressive deformation of different agglomerate types is also distinguishable.

The above experimental results show that, given the anisotropic characteristics emanating from printing layer directions, the agglomerate compression curves can successfully reveal the influence of sample print orientations and bond strength.

<Figure 9: Typical force-displacement curves under different test conditions >

<Figure 10: Force diagram of a single doublet under different test conditions >

<Figure 11: Shear and tensile strength of bonds between two primary particles>

3.2 Drop weight impact tests

The failure of the agglomerates under impact has been explored at different levels of impact stresses as mentioned before. The impact patterns of agglomerates are shown in Figures 12 and 13. High speed camera stills were used to illustrate the breakage process. Time zero indicates the first contact between the drop weight and the agglomerate. For all the impact tests, “loading direction 1” was used, i.e. the printed layers of the agglomerates are horizontal to the anvil (see Figures 5(a) and (c)).

Figure 12 shows the impact breakage patterns for agglomerates prepared in Print Orientations A and B, and tested according to conditions shown in Figures 5(a) and (c), respectively. In this test, the agglomerate type III was used, and the drop weight is 0.2 kg (1.6 J Impact energy). For “Print Orientation A” agglomerates under “loading direction 1”, the agglomerate fractured into three main fragments, and small fragments detached from the sides of the contact region (See Figure 12 a). For “Print Orientation B” case under “loading direction 1”, the agglomerate broke into two equal fragments through the meridian plane. As shown in Figure 12 b, the fracture surface is almost flat, and perpendicular to the anvil plane. Figure 12 clearly reveals different failure planes for the two print orientations loaded in direction 1: the “Print Orientation A” agglomerate fails through slip planes, whilst “Print Orientation B” agglomerate fail on cleavage planes.

<Figure 12: High speed camera recordings of impact-Agglomerate type III, 0.2 kg drop weight (1.6 J impact energy)>

Due to the increased impact energy with increased drop weight, the extent of breakage will be different. For the 0.2 kg drop weight (1.6 J impact energy) case, large fragments are formed and the failure plane is clearly distinguishable as shown in Figure 13 (a). As the drop weight increases, extensive shattering occurs, and the large fragments become weaker and break into small clusters as shown in Figure 13 (b). Figure 14 gives the impact-generated fragments of agglomerates of Figure 13. With increased impact energy, the amount of small debris increases and the size difference between the large fragment and small debris also increases. The extent of breakage ξ is determined by the following equation [20, 21]:

$$\xi = \frac{M_A - M_F}{M_A} \times 100 \tag{1}$$

where M_A is the mass of agglomerate, and M_F is the mass of largest fragment. The extents of breakage of agglomerates for both agglomerate type III and agglomerate type IV are shown in Figure 15. The results indicate that, for both cases, the increased impact energy has a significant effect on increasing the breakage extent of agglomerates. In addition, the agglomerate type III shows a higher breakage extent than the agglomerate type IV under the same test condition, which again makes intuitive sense.

<Figure 13: High speed camera recordings of impact for condition of Figure 5 (a) (Agglomerate type IV)>

<Figure 14: Fragments of agglomerates after impact breakage for condition of Figure 5 (a) (Agglomerate type IV)>

<Figure 15: Extent of breakage under different impact conditions for condition of Figure 5 (a)>

4. Discussion

Agglomerate breakage is a much more complex process to understand compared to the breakage of continuum solids. The 3D printed agglomerates tested in this study allowed us to conduct experiments on exact replica agglomerates, and to systematically vary a single factor (printing layer direction, applied load direction and bond strength) and study the results. This is the first time that such a systematic approach has been achievable experimentally, rather than being restricted to in silico simulations. The results in this initial study show that the mechanical properties of the inter particle bonds influence the deformation and the extent of impact breakage. In addition, the breakage is significantly influenced by different sample orientations, i.e. Print Orientations A and B as shown in Figure 5, which indicate that the relative printing position of bond network has a definitive effect on the breakage.

For compression tests under low strain rate, the compressive strength was significantly influenced by the bond strength and orientation effect. More specifically, the "Print Orientation A" samples deform along the slip planes ("45^o plane"), irrespective of the direction of load with regard to printing layer planes, and break at a high compressive load; whilst the "Print Orientation B" samples break easily through tensile stress on vertical planes, which resemble cleavage planes ("90^o plane"). In addition, the bond strength between primary particles is influenced by printing layer orientation and loading direction (see Figure 11), which implies that the inter-particle bond failure should be analysed in more detail in future. We plan to conduct further investigations to relate the microscopic particle-particle and particle-bond interactions to the macroscopic compressive breakage. For impact tests, clear failure planes of fractured agglomerates can be observed with low impact energy. As shown in Figure 12, under "loading direction 1", different failure planes are induced for different sample orientations: slip planes for "Print Orientation A" sample, and cleavage planes for "Print Orientation B" sample. At higher impact energy, a large amount of small debris is created, and the breakage extent increases accordingly. The results clearly reveal that the agglomerate breakage pattern is strongly dependent upon the sample print orientations: the “Print Orientation A” agglomerates fail through slip planes, whilst “Print Orientation B” agglomerates fail through vertical cleavage planes.

The above results show that the agglomerate breakage is controlled by a combination of the structure, bond properties and strain rate. DEM simulation is expected to be a useful tool to investigate the influence of these different factors on the macroscopic breakage mechanisms. Previously, simulation results generally struggled to match the experimental results for real agglomerates, especially for agglomerates with complex structure and irregular morphology [22]. The 3D printing method offers a possibility to precisely control the agglomerate structure and inter particle bond properties to investigate their influence on the agglomerate breakage and help to validate those DEM simulations. For a typical agglomerate design, multiple breakage tests can be performed at a range of strain rates and orientations to obtain a broad set of data representing the agglomerate strength distribution. After then, a corresponding DEM model with properties matching the ideal 3D printed agglomerate can be created, and the simulation results can be validated by the experimental data. However, most DEM simulations are based on simple adhesion bond models [23, 24]. This work shows clearly that more representative bond failure models as proposed by Potyondy & Cundall [25] and Brown et al. [26] are required. As part of an ongoing work, the simulations are in progress using the bonded particle contact models [26].

5. Summary

This paper has proposed a new method to produce agglomerates for breakage tests. The detailed production process includes computer aided design, 3D printing and the removal of support material. Based on this method, multiple agglomerates with desired properties and structure can be replicated which is helpful for investigations of agglomerate breakage. Compression and impact breakage tests were used to evaluate the performance of this method. The compression breakage tests showed good reproducibility at the same experimental conditions, and the influence of sample print orientations, loading directions and bond strength was addressed. The impact tests of agglomerates showed different breakage patterns in terms of sample orientations. For the fractured agglomerates, the extent of breakage increased with increasing impact energy. For both compression and impact test, the results show similar breakage patterns, i.e. failure on slip planes for “Print Orientation A”, and failure on vertical cleavage planes for “Print Orientation B”. The work reported here provides a rigorous approach for validating DEM simulations using realistic models of bond strength.

Acknowledgements

This research project was supported by International Fine Particle Research Institute (IFPRI) and an ARC Discovery grant (DP150100119). Ruihuan Ge’s PhD scholarship was supported by the China Scholarship Council (CSC). The authors would also like to acknowledge the assistance of Dr Donghai Yang at the University of Leeds for setting up the high speed video camera.

References

[1] Rumpf, H. (1958). Grundlagen und methoden des granulierens. Chemie Ingenieur Technik, 30(3), 144-158.

[2] Kendall, K. (1978). The impossibility of comminuting small particles by compression. Nature, 279(5709), 169–170.

[3] Rice, R. W. (1996). Grain size and porosity dependence of ceramic fracture energy and toughness at 22 °C. Journal of materials science, 31(8), 1969-1983.

[4] Smith, W. O., Foote, P. D., & Busang, P. F. (1930). Capillary retention of liquids in assemblages of homogeneous spheres. Physical Review, 36(3), 524.

[5] Manegold, E., Hofmann, R., & Solf, K. (1931). Ueber Kapillarsysteme XII. I. Die mathematische Behandlung idealer Kugelpackungen und das Hohlraumvolumen realer Gerüststrukturen. Colloid & Polymer Science, 56(2), 142-159.

[6] Meissner, H. P., Michaels, A. S., & Kaiser, R. (1964). Crushing strength of zinc oxide agglomerates. Industrial & Engineering Chemistry Process Design and Development, 3(3), 202-205.

[7] Farber, L., Tardos, G., & Michaels, J. N. (2003). Use of X-ray tomography to study the porosity and morphology of granules. Powder Technology, 132(1), 57-63.

[8] Rahmanian, N., Ghadiri, M., Jia, X., & Stepanek, F. (2009). Characterisation of granule structure and strength made in a high shear granulator. Powder Technology, 192(2), 184-194.

[9] Subero, J., Ning, Z., Ghadiri, M., & Thornton, C. (1999). Effect of interface energy on the impact strength of agglomerates. Powder Technology, 105(1), 66-73.

[10] Thornton, C., & Liu, L. (2004). How do agglomerates break? Powder Technology, 143, 110-116.

[11] Ghadiri, M., Moreno-Atanasio, R., Hassanpour, A., & Antony, S. J. (2007). Analysis of agglomerate breakage. Handbook of Powder Technology, 12, 837-872.

[12] Golchert, D. J., Moreno, R., Ghadiri, M., Litster, J., & Williams, R. (2004). Application of X-ray microtomography to numerical simulations of agglomerate breakage by distinct element method. Advanced Powder Technology, 15(4), 447-457.

[13] Golchert, D., Moreno, R., Ghadiri, M., & Litster, J. (2004). Effect of granule morphology on breakage behaviour during compression. Powder Technology,143, 84-96.

[14] Moreno-Atanasio, R., Williams, R. A., & Jia, X. (2010). Combining X-ray microtomography with computer simulation for analysis of granular and porous materials. Particuology, 8(2), 81-99.

[15] Dadkhah, M., Peglow, M., & Tsotsas, E. (2012). Characterization of the internal morphology of agglomerates produced in a spray fluidised bed by X-ray tomography. Powder Technology, 228, 349-358.

[16] Dadkhah, M., & Tsotsas, E. (2014). Study of the morphology of solidified binder in spray fluidised bed agglomerates by X-ray tomography. Powder Technology, 264, 256-264.

[17] Subero, J., & Ghadiri, M. (2001). Breakage patterns of agglomerates. Powder Technology, 120(3), 232-243.

[18] Mishra, B. K., & Thornton, C. (2001). Impact breakage of particle agglomerates. International Journal of Mineral Processing, 61(4), 225-239.

[19] PolyJet Materials, available online at http://www.stratasys.com/materials/polyjet

[20] Samimi, A., Moreno, R., & Ghadiri, M. (2004). Analysis of impact damage of agglomerates: effect of impact angle. Powder technology, 143, 97-109.

[21] Subero-Couroyer, C., Ghadiri, M., Brunard, N., & Kolenda, F. (2005). Analysis of catalyst particle strength by impact testing: The effect of manufacturing process parameters on the particle strength. Powder technology, 160(2), 67-80.

[22] Golchert, D. J., PhD Thesis, The University of Queensland, Queensland, Australia, 2003.

[23] Johnson, K. L., Kendall, K., & Roberts, A. D. (1971, September). Surface energy and the contact of elastic solids. In Proceedings of the Royal Society of London A: Mathematical, Physical and Engineering Sciences (Vol. 324, No. 1558, pp. 301-313). The Royal Society.

[24] Thornton, C., & Yin, K. K. (1991). Impact of elastic spheres with and without adhesion. Powder technology, 65(1), 153-166.

[25] Potyondy, D. O., & Cundall, P. A. (2004). A bonded-particle model for rock. International journal of rock mechanics and mining sciences, 41(8), 1329-1364.

[26] Brown, N. J., Chen, J. F., & Ooi, J. Y. (2014). A bond model for DEM simulation of cementitious materials and deformable structures. Granular Matter, 16(3), 299-311.

Figure 1: 3D printing process showing the printer, the software arranging the models to be printed, and the final product on the build tray.

Figure 2: Schematic drawing of doublet.

Figure 3: Agglomerate design in terms of different orientations.

Figure 4: Removal of support materials

Figure 5: Different test directions and sample orientations used in breakage tests

Figure 6: Schematic of breakage test setups

Figure 7: Force-displacement curves of agglomerates for condition of Figure 5 (a) (Agglomerate type I)

Figure 8: Force-displacement curves of agglomerates for condition of Figure 5 (c) (Agglomerate type I)

Figure 9: Typical force-displacement curves under different test conditions

Figure 10: Force diagram of a single doublet under different test conditions

Figure 11: Shear and tensile strength of bonds between two primary particles

Figure 12: High speed camera recordings of impact-Agglomerate type III, 0.2 kg drop weight (1.6 J impact energy)

Figure 13: High speed camera recordings of impact for condition of Figure 5 (a) (Agglomerate type IV)

Figure 14: Fragments of agglomerates after impact breakage for condition of Figure 5 (a) (Agglomerate type IV)

Figure 15: Extent of breakage under different impact conditions for condition of Figure 5 (a)

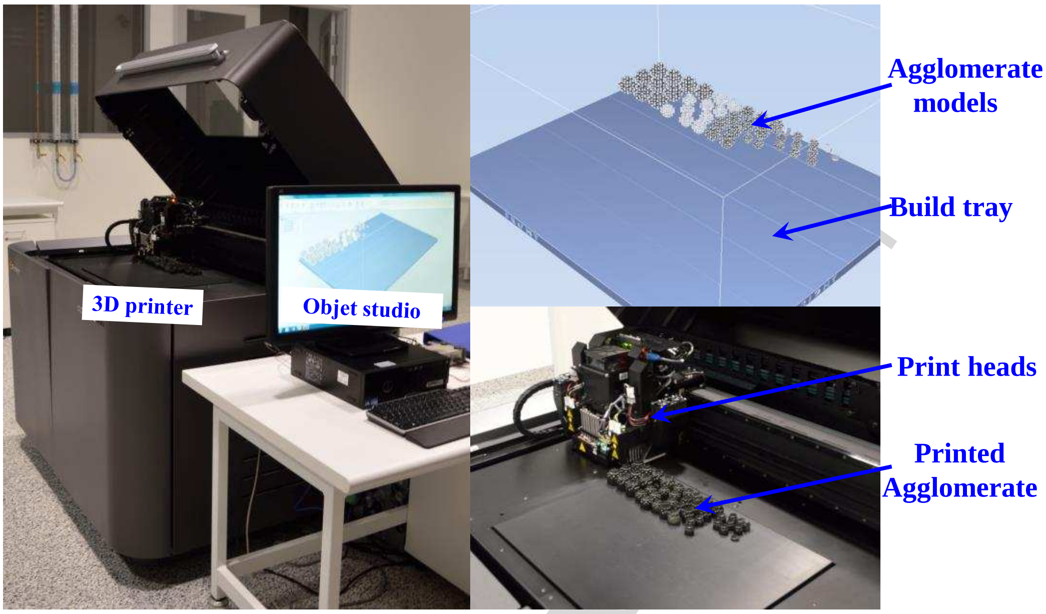

Figure 1: 3D printing process showing the printer, the software arranging the models to be printed, and the final product on the build tray.

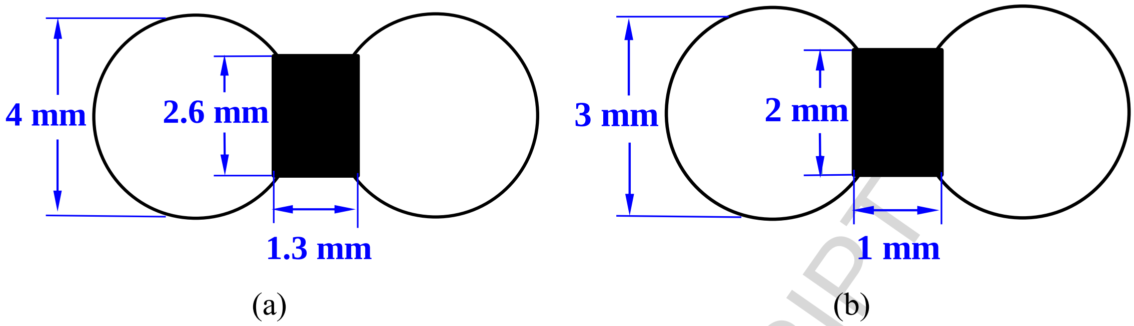

Figure 2: Schematic drawing of doublet.

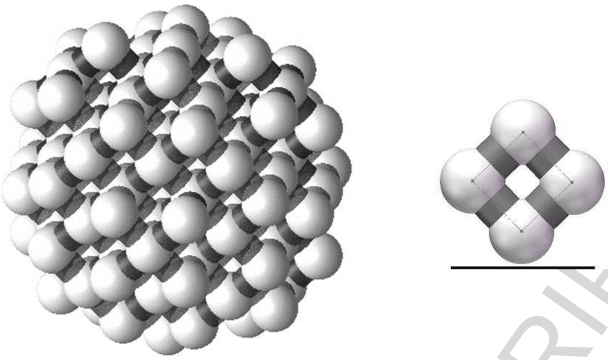

(a) Print Orientation A

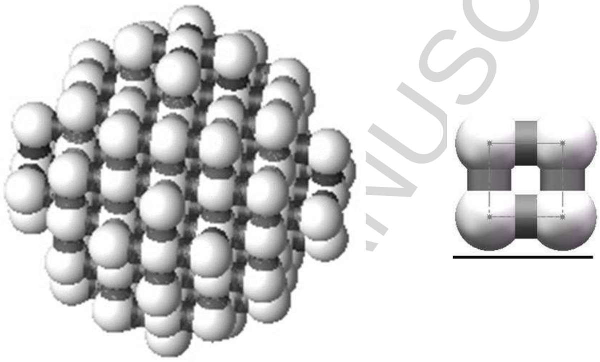

(b) Print Orientation B

Figure 3: Agglomerate design in terms of different printing orientations.

(a) (b)

Figure 4: Removal of support materials (a) printed agglomerates showing support material under the overhangs (b) various finished and cleaned agglomerates.

	Loading direction 1	Loading direction 2
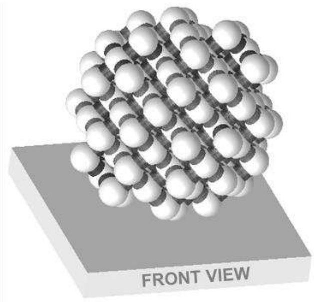 **Print Orientation A**	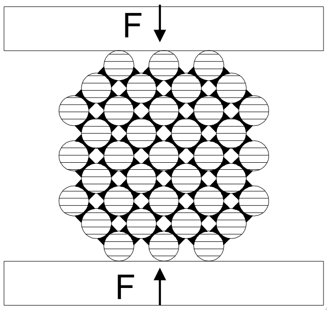 **(a)**	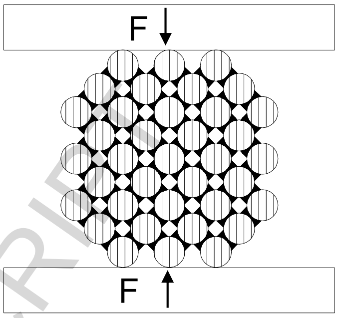 **(b)**
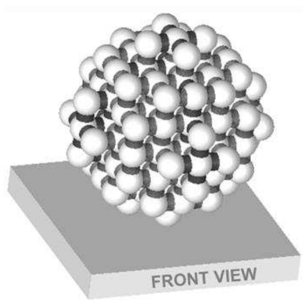 **Print Orientation B**	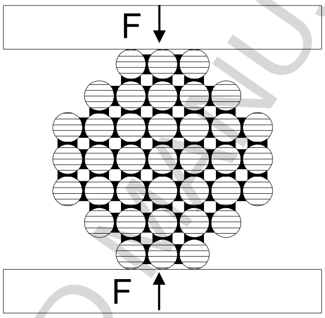 **(c)**	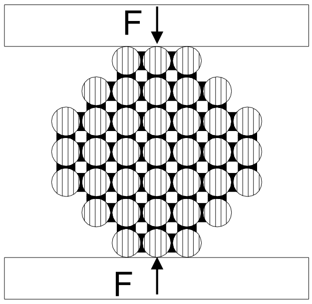 **(d)**

Figure 5: Different test directions and sample orientations used in breakage tests. Hatch lines within the particles indicate the direction of the 3D print layers.

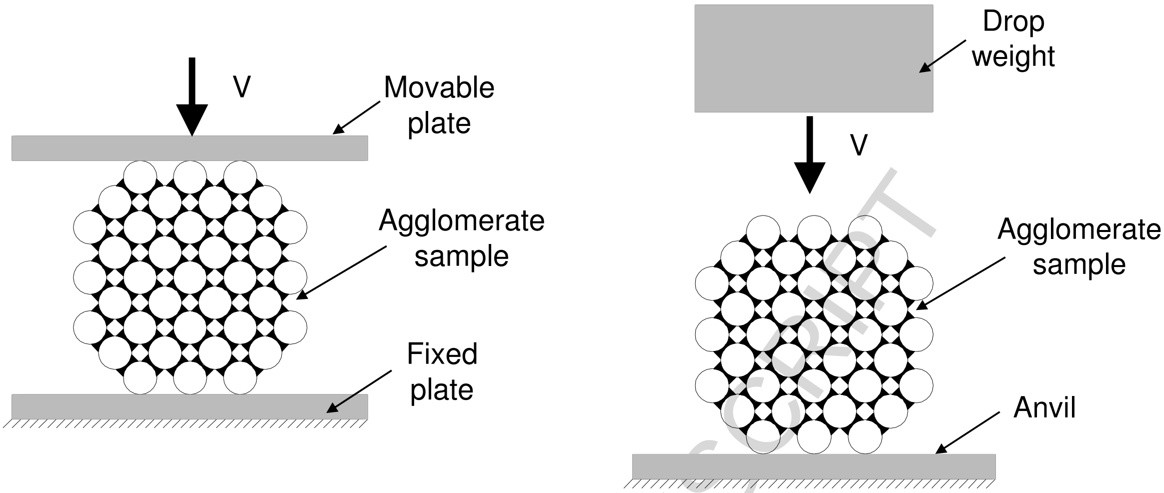

(a) Compression test (b) Drop weight impact test

Figure 6: Schematic of breakage test setups

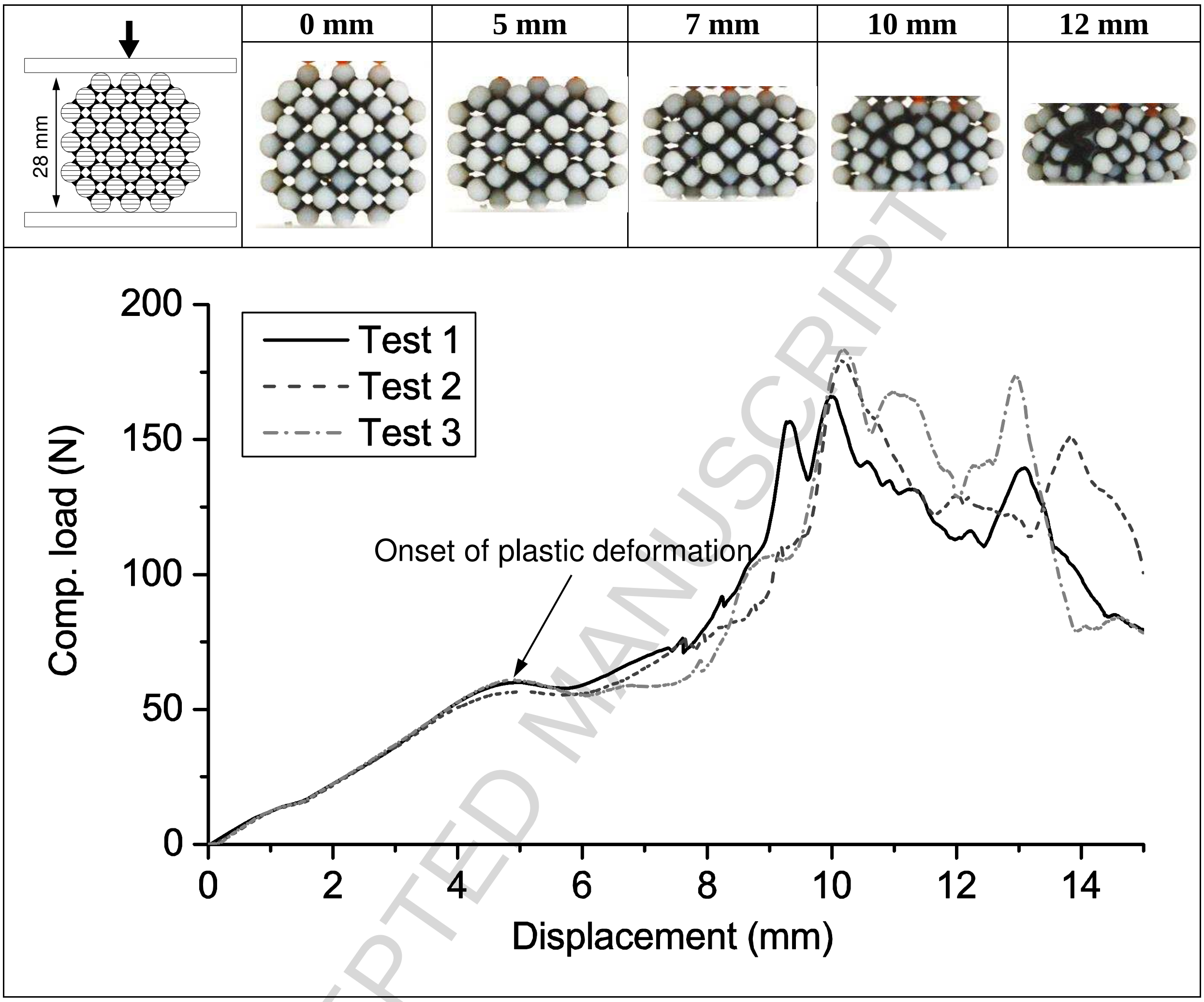

Figure 7: Force-displacement curves of agglomerates for condition of Figure 5 (a) (Agglomerate type I)

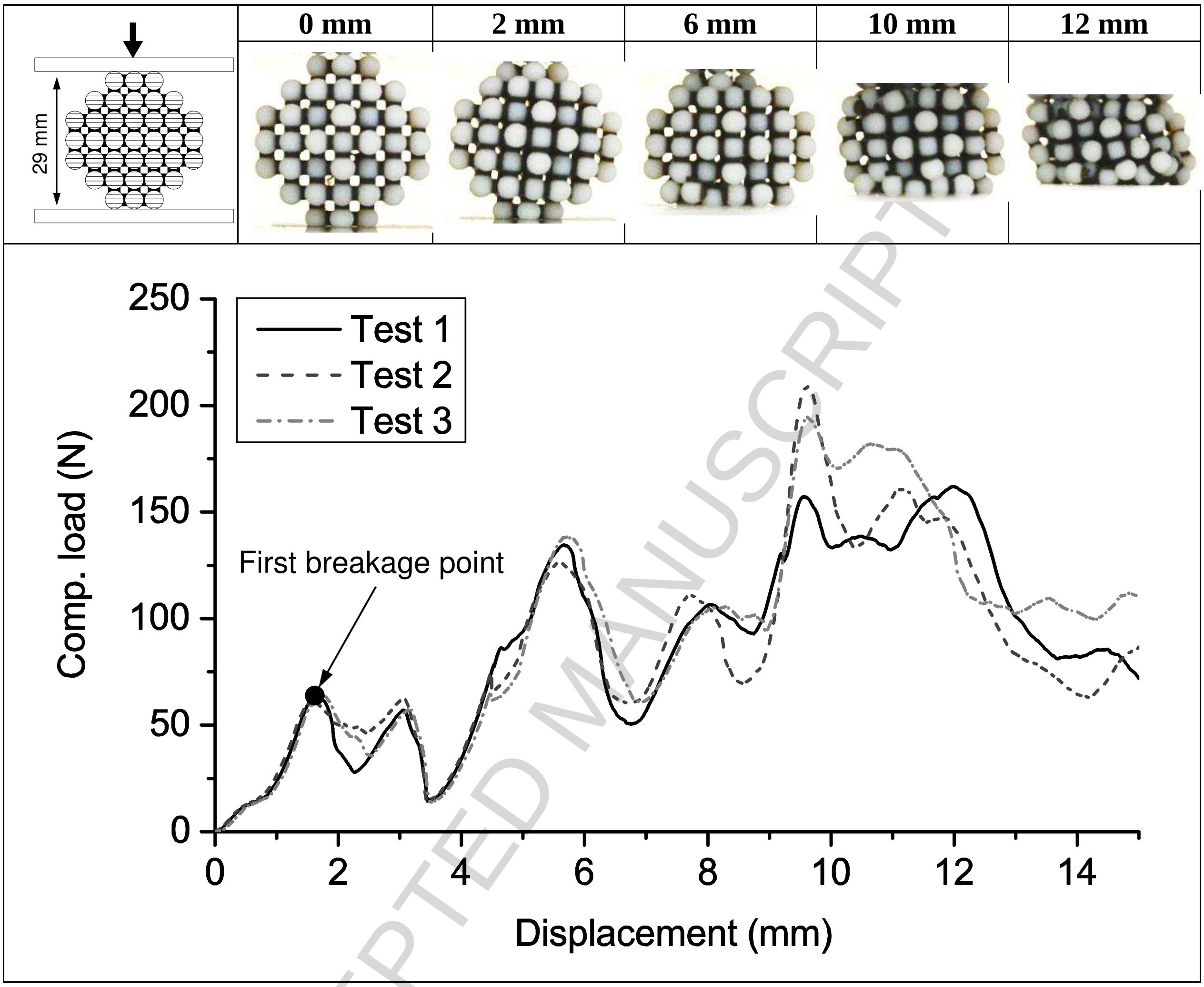

Figure 8: Force-displacement curves of agglomerates for condition of Figure 5 (c) (Agglomerate type I)

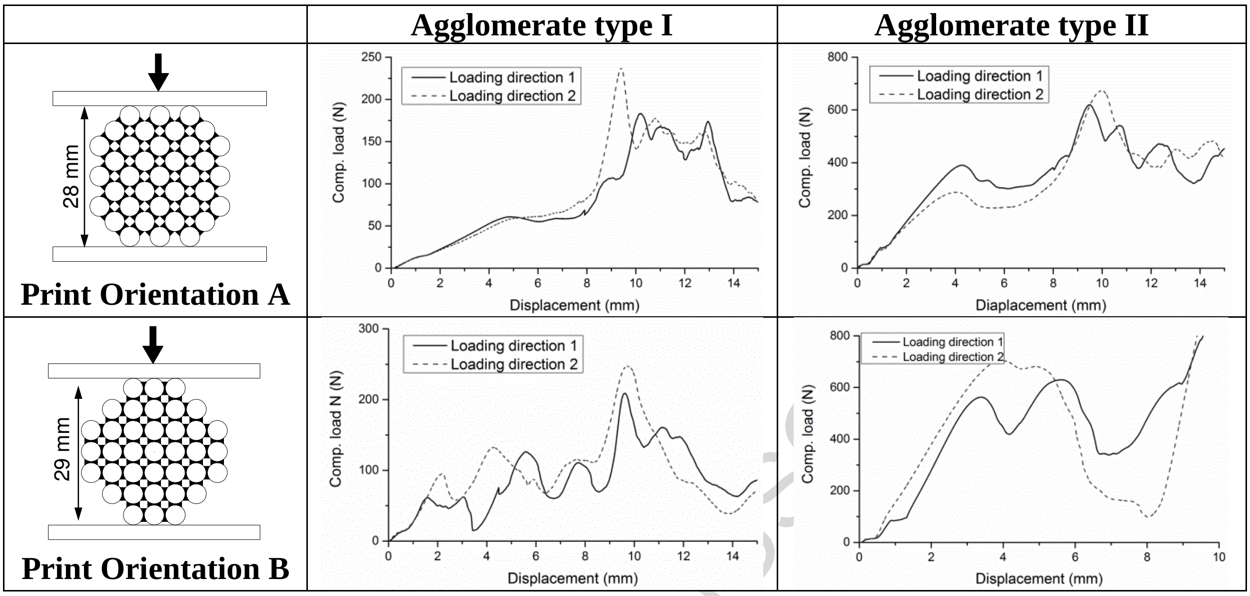

Figure 9: Typical force-displacement curves under different test conditions

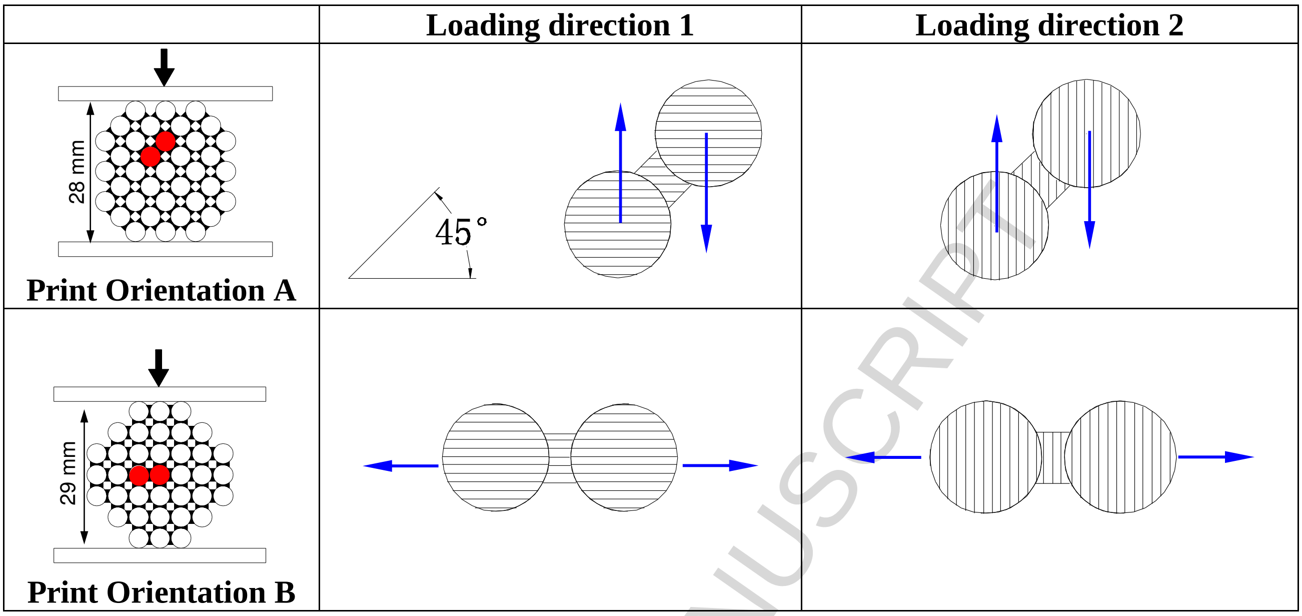

Figure 10: Force diagram of a single doublet under different test conditions

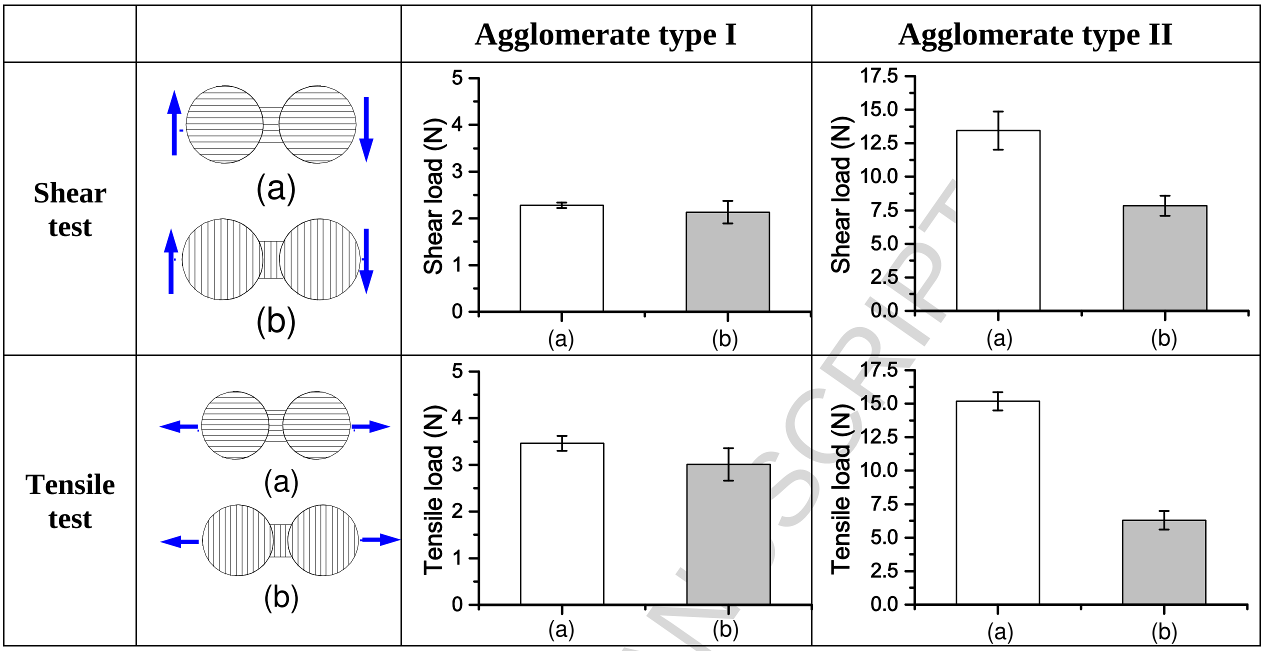

Figure 11: Shear and tensile strength of bonds between two primary particles

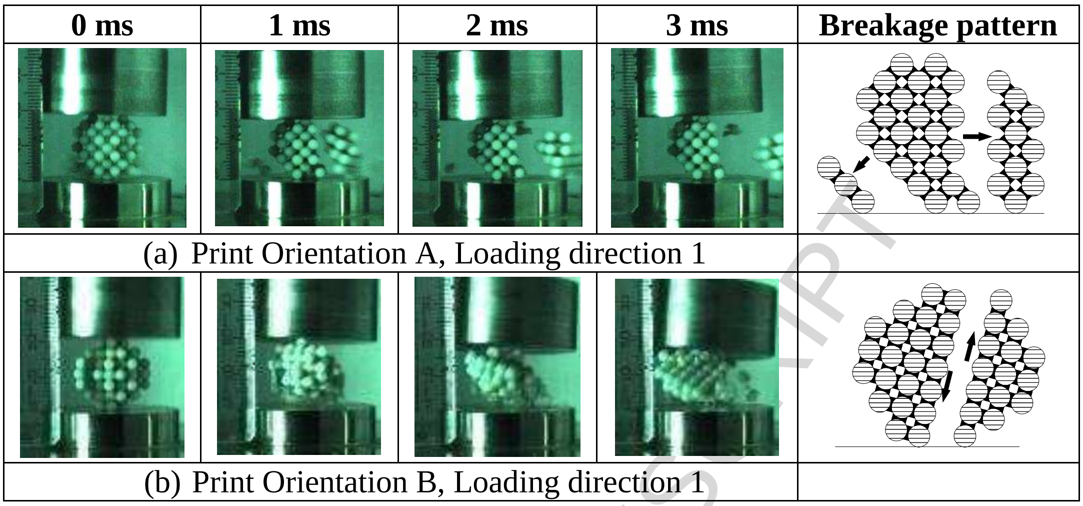

Figure 12: High speed camera recordings of impact-Agglomerate type III, 0.2 kg drop weight (1.6 J impact energy)

0 ms	1 ms	2 ms	3 ms
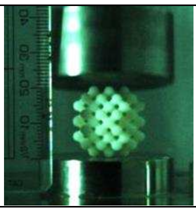	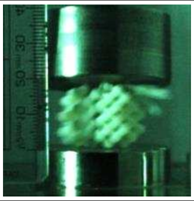	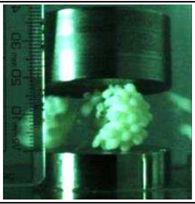	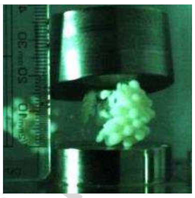
(a) 0.2 kg drop weight (1.6 J impact energy)			
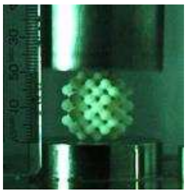			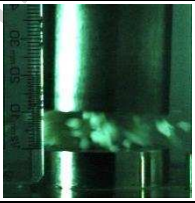
(b) 0.6 kg drop weight (4.8 J impact energy)			

Figure 13: High speed camera recordings of impact for condition of Figure 5 (a) (Agglomerate type IV)

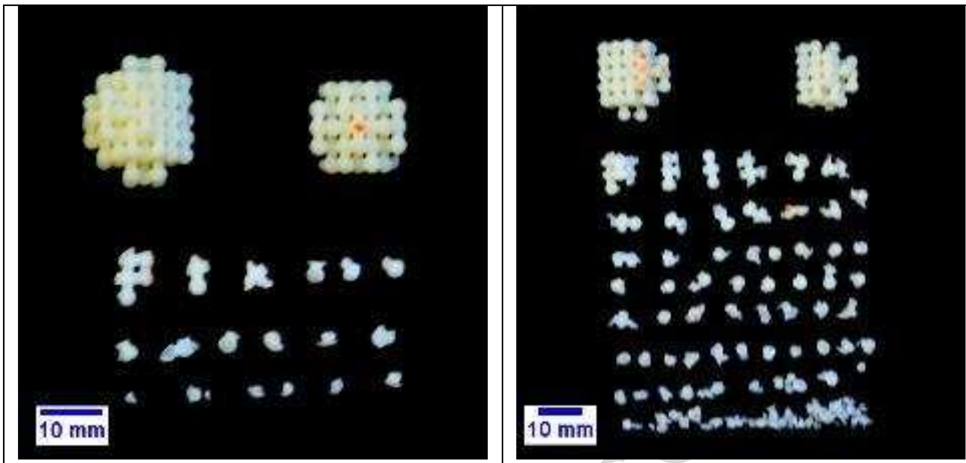

(a) 0.2 kg drop weight (1.6 J impact energy)	(b) 0.6 kg drop weight (4.8 J impact energy)

Figure 14: Fragments of agglomerates after impact breakage for condition of Figure 5 (a) (Agglomerate type IV)

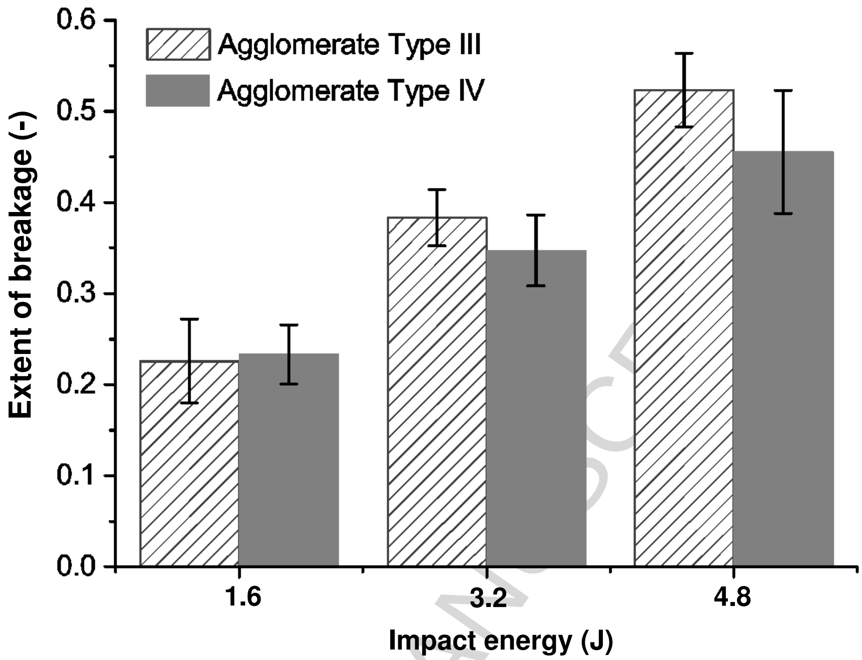

Figure 15: Extent of breakage under different impact conditions for condition of Figure 5 (a)

Tables:

Table 1: Mechanical properties of 3D printing polymer materials

Table 2: Parameters of the tested agglomerates

Table 1: Mechanical properties of 3D printing polymer materials

Material name	Tensile strength (MPa)	Shore hardness[1]	Elasticity modulus (MPa)
DM 9840	1.3-1.8	35-40 (A)	-
DM 9895	8.5-10.0	92-95 (A)	-
DM 8530	35-45	79.5-83.5 (D)	1400-2000
Vero WhitePlus™	50-65	83-86 (D)	2000-3000

[1]A and D are the two most common scales (ASTM D2240). The A scale is for softer plastics, while the D scale is for harder ones.

Table 2: Parameters of the tested agglomerates

Agglomerate type[1]	Primary particle material	Primary particle size	Bond material
I	Vero WhitePlus™	4 mm	DM 9840
II			DM 9895
III		3 mm	DM 8530
IV			Vero WhitePlus™

[1]Agglomerate type I and type II were used during compression tests, while agglomerate type III and type IV were used during impact tests.

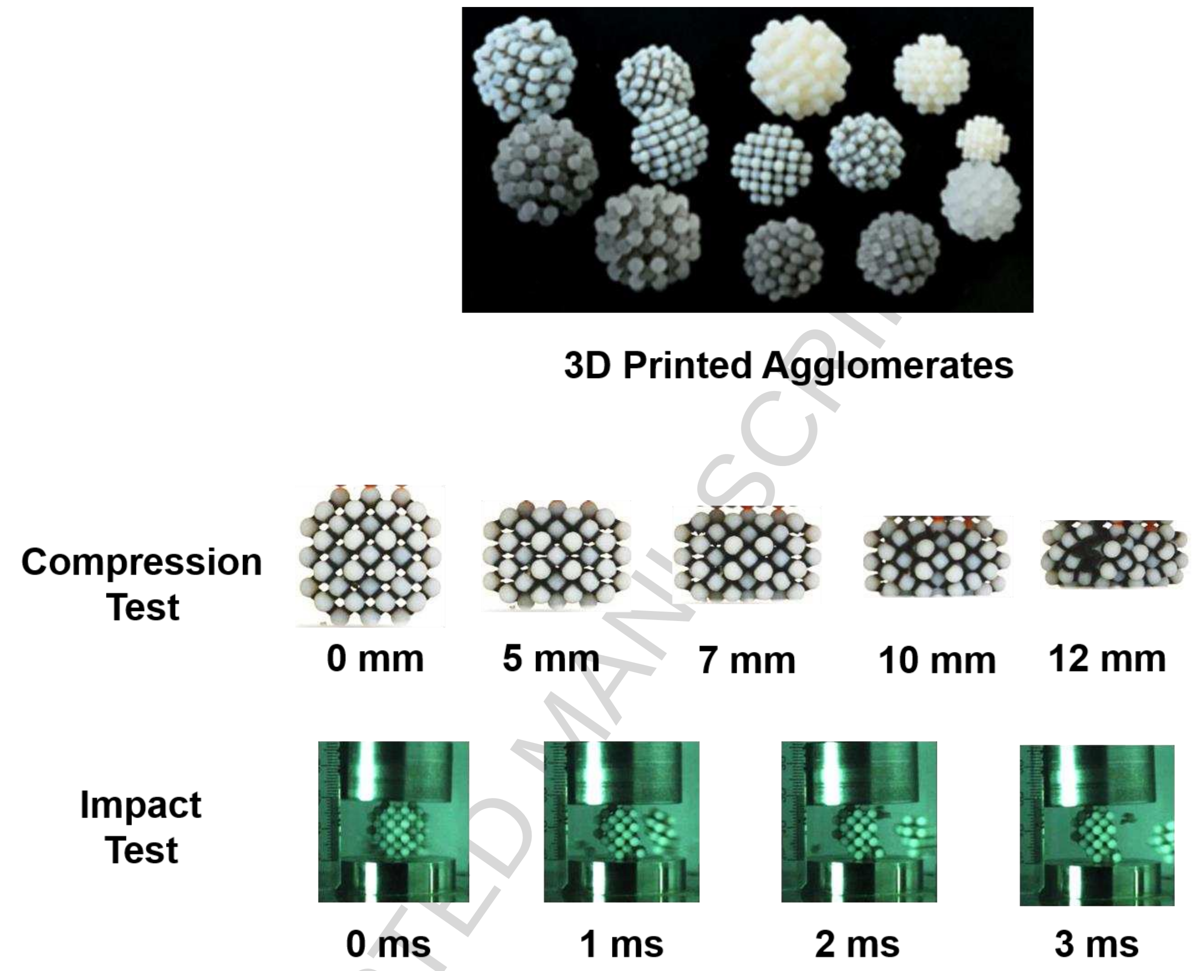

Graphical abstract

Highlights

- A novel method of producing test agglomerates was presented.
- Compression and impact tests were performed to investigate the agglomerate breakage.
- The effects of sample orientations, loading directions and bond strength on the breakage behaviour were addressed.
- This new method will allow more rigorous testing of agglomerate breakage models.